Silicon (2018) 10:1225–1230
https://doi.org/10.1007/s12633-017-9596-z

ORIGINAL PAPER

Synthesis of Nano-Structured Strontium Titanate by Sol-Gel and Solid State Routes

A. M. Youssef[1] · H. K. Farag[1] · A. El-Kheshen[2] · F. F. Hammad[1]

Received: 10 February 2017 / Accepted: 2 June 2017 / Published online: 30 September 2017

Abstract In this paper strontium titanate $SrTiO_3$ nanopowders were synthesized via sol-gel and solid state methods with the aim of exploring the influence of the synthesis process on the obtained material. $SrTiO_3$ powders were characterized by different spectroscopic and microscopic techniques, such as x-ray diffraction (XRD), infrared (IR), thermogravimetric analysis (TGA) and differential thermal analysis (TGA-DTA), scanning electron microscopy (SEM) and transmission electron microscopy (TEM). The magnetization and the dielectric characteristics of the synthesized $SrTiO_3$ were demonstrated. XRD results revealed the formation of $SrTiO_3$ and $SrTiO_3$ with anatase TiO_2 by solid state and sol-gel methods, respectively. The synthesis of $SrTiO_3$ by the solid state route led to the formation of microcrystalline particles. However, the sample prepared by the sol-gel method was more homogenous containing very fine particles with sizes in the nanometer regime. The TEM investigation showed the formation of nanoparticles with an average size of about 10 nm. The sol-gel synthesized sample exhibited a higher magnetization compared with the solid state synthesized one. The values of the dielectric of constants sol-gel synthesized samples are higher than those of the samples prepared by the solid state method.

✉ H. K. Farag
msherif888@yahoo.com

[1] Inorganic Chemistry Department, National Research Centre, El Behoth St. 33, Dokki, Giza, Egypt

[2] Glass Department, National Research Centre, El Behoth St. 33, Dokki, Giza, Egypt

Keywords Strontium titanate · Thermoelectric materials · Perovskite · Nanoparticles · Sol-gel synthesis · Ceramic sample

1 Introduction

Perovskite compounds have been generating tremendous interest due to their structure and importance in opto-electronic devices and in host fluorescence materials. Among the perovskites, thermoelectric materials have attracted considerable attention for their potential application in power generation devices that are designed to convert waste heat into electrical energy. Perovskite strontium titanate $SrTiO_3$ (STO) is one of the most important thermoelectric materials, which has a high potential for use in thermoelectric generators in which thermal energy is converted directly into electrical energy. STO is an important n-type semiconductor with a band gap of 3.2 eV and has a large Seebeck coefficient [1]. Moreover, STO has a high photocatalytic activity, high static dielectric constant, low dielectric loss, high nonlinear optical coefficient [2, 3] and good insulation [4]. $SrTiO_3$ is also an attractive material for application in microelectronics because of its excellent optical transparency in the visible region and high charge storage capacity [5]. Several techniques have been reported for the synthesis of $SrTiO_3$ nanoparticles such as sputtering [6, 7], sol-gel [8–10], laser ablation [11, 12], micro-emulsion [13], hydrothermal co-precipitation [14, 15] and combustion method [16]. It is well known that the structure and composition of nanomaterials depend on the synthesis method.

In this work we focus on the synthesis and characterization of cubic perovskite $SrTiO_3$ via a sol-gel method using $SrCl_2$ and $TiCl_4$ as starting materials. The sol-gel process

is a well known chemical synthetic mechanism involving the formation of an amorphous gel from a precursor solution. The sol-gel method is a commonly used method for the synthesis of such oxides. Metal chlorides are suitable starting materials for sol-gel reactions as they are available in high purity. The perovskite $SrTiO_3$ was also synthesized via a solid state method using SrO and TiO_2 as precursors. The influence of the synthesis process on the structure, morphology and crystallite size of the synthesized oxide was explored.

Normally, the chemical solution methods, in general, and the sol-gel method, in particular, produce more homogeneous, finer particle size and higher purity of the synthesized powders than that prepared by the solid state method. However, the solid state method shows some advantages such as the use of low cost raw materials and the simplicity of the synthesis procedure. The oxide precursors, TiO_2 and SrO, used for the synthesis of $SrTiO_3$ by the solid state route are comparatively cheaper than the chloride/alkoxide salts, which are usually used for the wet chemical routes. In the present study, two synthesis approaches, sol-gel and solid state, were employed for the synthesis of $SrTiO_3$ with the aim of exploring the influence of the synthesis process on the obtained material. Various spectroscopic and microscopic techniques were used to characterize the synthesized $SrTiO_3$ powders, such as XRD, IR, TGA-DTA, SEM and TEM. The magnetization of the synthesized $SrTiO_3$ with respect to a magnetic field was demonstrated. The dielectric characteristics were also investigated.

2 Experimental

$SrTiO_3$ was synthesized via a sol-gel method in isopropanol (Alfa, 99.5%) using $SrCl_2$ (Alfa, 99%) and $TiCl_4$ (Alfa, 99%) as precursors. Distilled water was used for hydrolysis of the precursor solution, ammonium hydroxide (Sigma Aldrich 98%) was used to adjust the pH. The synthesized samples were calcined in a muffle oven at the desired temperature for 2 h and were cooled down to the ambient temperature in the oven. $SrTiO_3$ was also synthesized via a solid state method using SrO and TiO_2 with purity of about 98% as precursors. The morphology and particle size of the as prepared samples were investigated by a high resolution scanning electron microscope (FEI Quanta 250 FEG) and a transmission electron microscope (TEM, JEM/1230 model, Japan). The phase composition of the as-prepared and calcined samples was investigated using a Philips - diffractometer Model PW 2013, Netherlands, operating at 35 kV and 20 mA with a source of CuK_α radiation. The main functional surface groups of the prepared samples were determined by Fourier transform infrared spectroscopy FTIR using KBr pellets JASCO, FT/IR 460 plus. Thermal gravimetric analysis (TGA) and differential thermal analysis (DTA) were carried out by a Universal V4.7 TA-Instruments analyzer at a heating rate of 10 °C /min. starting from room temperature up to 1000 °C in air. A computerized LRC Bridge (Hioki model 3532-50 LCR Hi Tester) was used to measure the dielectric constants for the synthesized samples in the temperature range from 50 to 400 °C, in the frequency range from 42 Hz to 5 MHz. The measurements were performed after sufficient time at each temperature for establishing equilibrium values. A Vibrating Sample Magnetometer, VSM Lakeshore 7410 USA, was used for magnetic property measurements with a maximum applied field of ±1.9 kOe.

3 Results and Discussion

3.1 Preparation of $SrTiO_3$

For sol-gel method, a solution of 1 M $CaCl_2$ and 1 M $MnCl_2$ in isopropanol was prepared and hydrolyzed by addition of an appropriate amount of water. The solution was maintained under stirring in order to form a gel. The pH was then adjusted at 8 by a dropwise addition of ammonium hydroxide and stirring maintained. After that, the mixtures were centrifuged to regain the product.

For the synthesis of $SrTiO_3$ by the solid state method, stoichiometric quantities of the analytical graded precursors SrO and TiO_2 were mixed and well-milled in a vibratory ball mill. Then the mixed powders were uniaxially pressed at 60 MPa in a disc shape of about 1/2 inch in diameter and height. The pressed sample was calcined at a temperature of 1300 °C for 10 h.

3.2 Characterization of the Synthesized Oxide

The synthesized powder was characterized by XRD, SEM and TEM to investigate the composition and the particle size of the produced oxide. Figure 1 shows the XRD patterns of the oxide powders obtained by sol-gel and solid state methods. The XRD patterns of the sample synthesized by sol-gel shows, in addition to the characteristic peaks of strontium titanate ($SrTiO_3$), the peaks of anatase TiO_2. The recorded peaks of $SrTiO_3$ are well indexed according to the JCPDS (PDF-01-089-4934) card and the peaks of TiO_2 correspond to the data available for the anatase phase in the JCPD 21-1272 diffraction file. This suggests the formation of $SrTiO_3$ along with the formation of anatase TiO_2 crystals.

The XRD pattern of strontium titanate prepared by solid state shows the formation of a well-crystallized strontium titanate single phase without impurity phases such as strontium or titanium oxides, starting materials used for preparation. The main peak is found at 32.37°, corresponding to the (110) plane of strontium titanate perovskite structure,

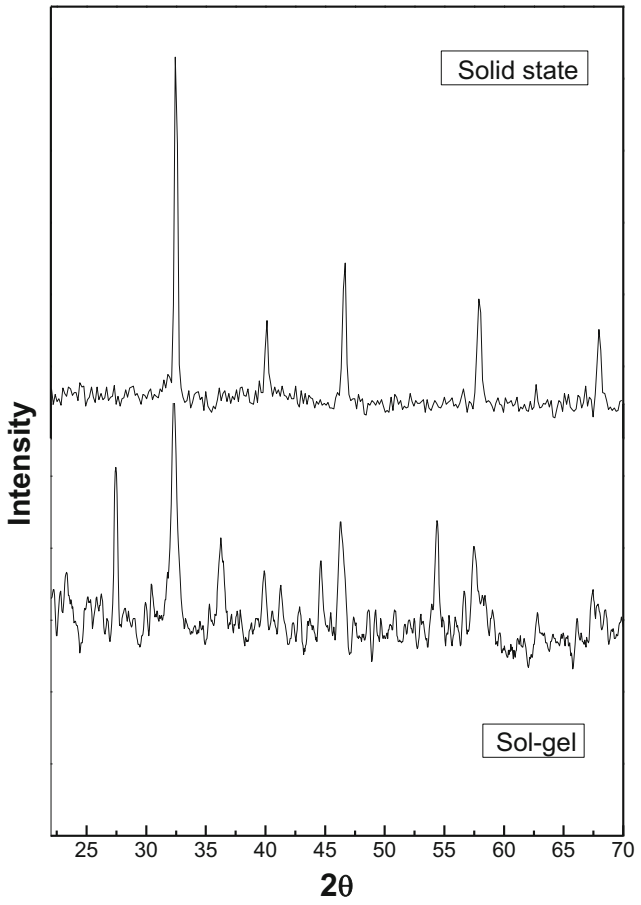

Fig. 1 XRD patterns of strontium titanate prepared by sol-gel and by solid state

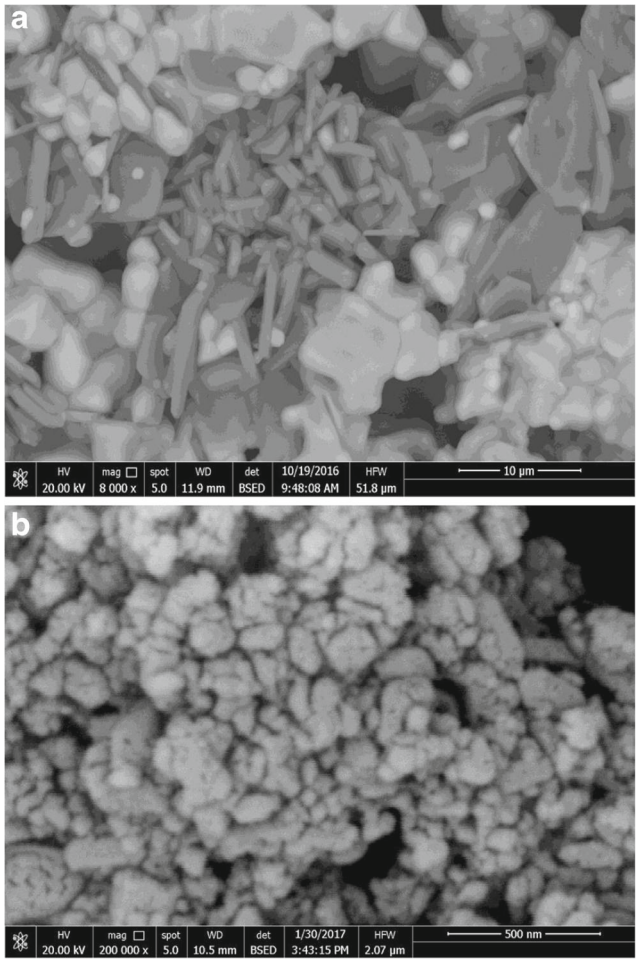

Fig. 2 SEM micrograph of the synthesized $SrTiO_3$ prepared by solid state method

confirming that the grains are preferably orientated along the (110) plane.

For sintered ceramic materials, it is important to investigate the microstructure which gives a better insight on the grain-grain interactions, morphology of the grains, and material density i.e. the amount of porosity and the size of pores. Consequently, the microstructure can reflect and affect all properties of materials.

The sample prepared by the sol-gel and solid state methods were characterized by means of high resolution field emission scanning electron microscopy (SEM). The SEM micrographs of Fig. 2 present the morphology of the obtained oxide. As can be seen, the prepared $SrTiO_3$ includes heterogeneous particles with sizes in the micrometer regime, Fig. 2a. This indicates the synthesis of $SrTiO_3$ by the solid state route leads to the formation of microcrystalline particles. However, the sample prepared by the sol-gel method is more homogenous as very fine particles with sizes in the nanometer regime are obtained, Fig. 2b. This reveals the formation of nanostructured $SrTiO_3$ by the sol-gel method.

The synthesized samples were further characterized by TEM in order to get a reliable insight into the particle size of the obtained oxides. The TEM micrographs of the solid state and sol-gel synthesized samples are shown in Fig. 3. As seen, the solid state synthesized sample shows coarse particles, Fig. 3a, whereas the sol-gel synthesized oxide comprises nearly spherical, very fine particles with an average size of about 10 nm, Fig. 3b.

The FTIR spectra of the prepared samples are presented in Fig. 4. The basic functional groups present in the prepared sample were determined qualitatively by FTIR analysis. As can be seen $SrTiO_3$ exhibits some characteristic absorption bands: a broad band at ~3400 cm^{-1} due to O-H stretching of adsorbed water molecules and surface hydroxyl groups, bands at 1004, 1354 cm^{-1} due to the use of alcohol in the preparation process, and a strong and wide band located between 800 and 500 cm^{-1} owing to $SrTiO_3$ stretching vibrations confirming the formation of $SrTiO_3$.

The differential thermal analysis and thermogravimetric analysis DTA-TGA curves of the $SrTiO_3$ sample are displayed in Fig. 5. The TGA curve can be generally divided into three major processes: the first one is observed in the

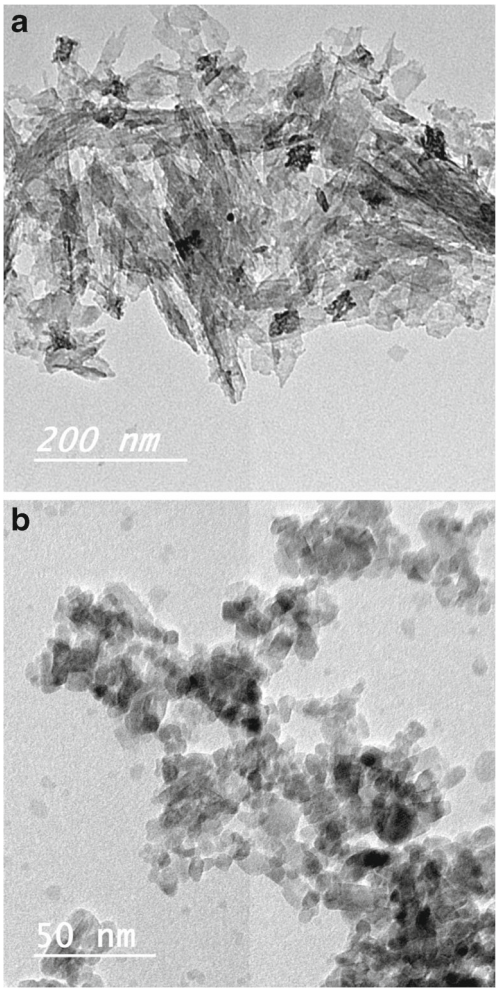

Fig. 3 TEM micrographs of $SrTiO_3$ prepared by sol-gel method

temperature range from 35–300 °C, with a weight loss of about 15%, which can be correlated to the evaporation of

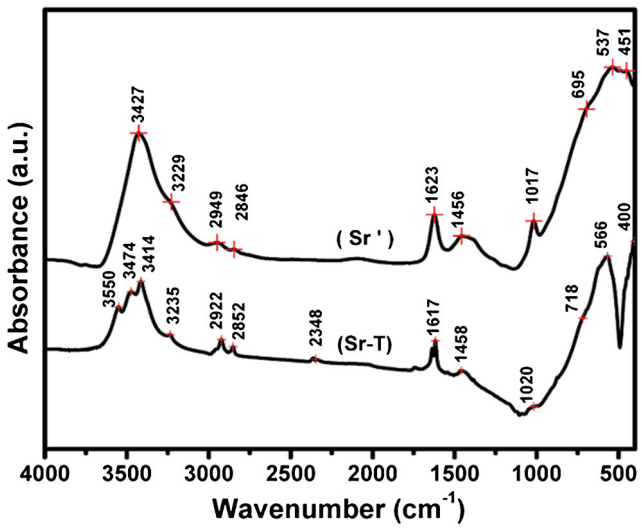

Fig. 4 FTIR spectra of $SrTiO_3$ prepared by so-gel and by solid state

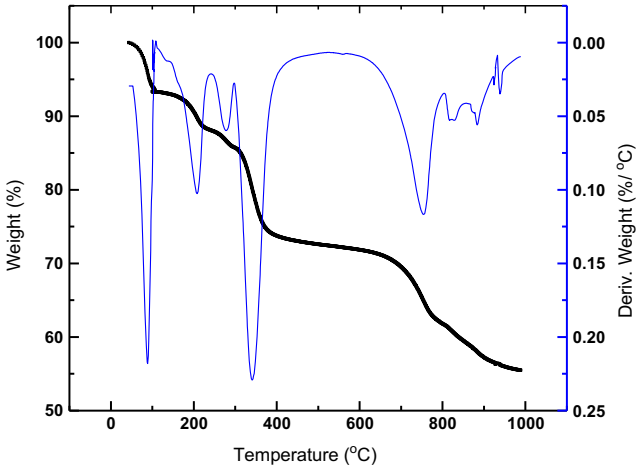

Fig. 5 TGA-DSC curves of $SrTiO_3$ prepared by sol-gel method

physically adsorbed water (dehydration). The corresponding DTA peaks are observed at 88, 205 and 275 °C. The second process is from 300–400 °C where a significant mass loss of about 12% is observed, which might be attributed to removal of organic residues. A strong DTA peak is recorded at 340 °C. In the third process from 700 to 1000 °C a mass loss of about 13% is observed as a result of removal of the surface hydroxyls (dehydroxylation) and/or evaporation of chemisorbed water. A significant DTA peak is observed at 750 °C.

3.3 Magnetic Measurements

The magnetic properties of the synthesized oxides were investigated. Figure 6 shows the magnetization curves of $SrTiO_3$ obtained by both solid state, Fig. 6a, and sol-gel methods, Fig. 6b, as a function of the magnetic field. As shown in Fig. 6 the hysteresis loops of the obtained samples exhibit an "S" shape which is typical for soft magnetic materials.

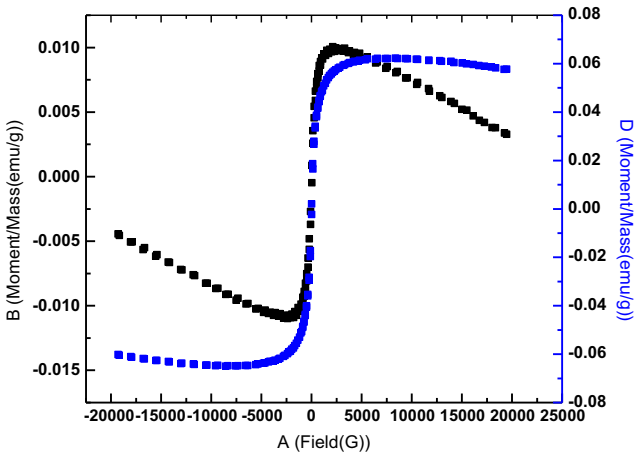

Fig. 6 Magnetic hysteresis loop (M-H) of the synthesized $SrTiO_3$

The sol-gel synthesized sample exhibits a higher magnetization compared with the solid state synthesized one. A lower value of magnetisation in the solid state synthesized sample, compared with that of the sol-gel sample, might indicate a lowering of a cation distribution factor. The hysteresis curves at low applied fields exhibit the values of the coercive field, $H_c = 24$ G for the solid state synthesized sample and 13.77 G for the sol-gel synthesized sample. The remnant magnetization (M_r) is 2.05×10^{-3} emu/g and 0.638×10^{-3} emu/g for the sol-gel and solid state synthesized samples, respectively.

3.4 Dielectric Measurements

The dielectric function (constant), ε' of $SrTiO_3$, synthesized by both solid state and sol-gel methods, was calculated from the measured capacitance ($\varepsilon' = C_p d/\varepsilon_0 A$) at a frequency range of 50 Hz–5 MHz and a temperature range of 25–400 °C. The variation of the dielectric constant and dielectric loss of the sol-gel and of solid state synthesized samples as a function of frequency and temperature are depicted in Figs. 7 and 8, respectively. It is clearly seen that the dielectric constant and dielectric loss of the sample sintered at different temperatures decrease with the increase in frequency. The dielectric constant for the sample sintered at 400 °C shows a higher value compared with those of the samples sintered at other temperatures, Fig. 7a. This means the condition of the samples are in the most optimized state and that should be suitable for the applications.

The dielectric relaxation peaks in the dissipation factor appeared at frequency >1 kHz and shifted towards a higher frequency with the increase in sintering temperature. It is suggested that the appearance of relaxation peaks is due to the movement of oxygen ions or oxygen vacancies [17]. The samples sintered at 400 °C showed higher values of dielectric constant with lower values of loss tangent along with higher density.

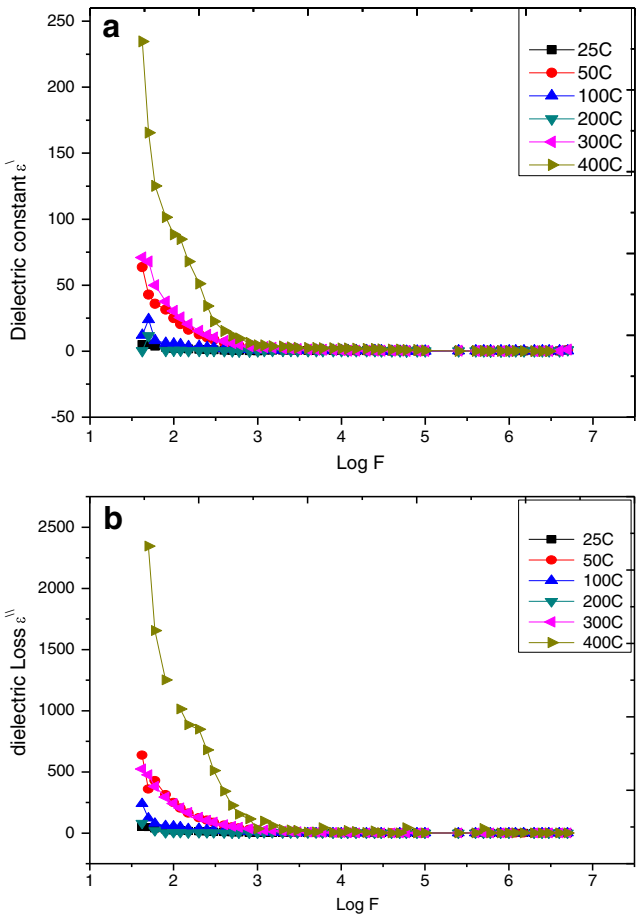

Fig. 7 Variation of dielectric constant, **a**, and of the dielectric loss, **b**, of the solid state synthesized $SrTiO_3$ as a function of frequency at different temperatures

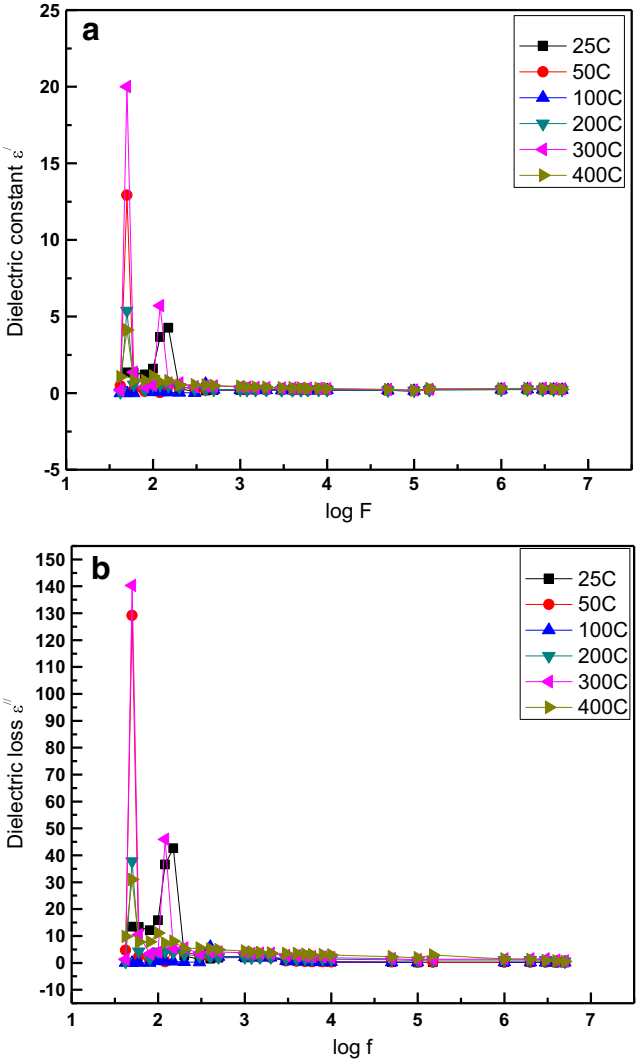

Fig. 8 Variation of dielectric constant, **a**, and of the dielectric loss, **b**, of the sol-gel synthesized $SrTiO_3$ as a function of frequency at different temperatures

The large values of the dielectric constant at low frequency may be an indication of spontaneous polarization [18]. At low frequencies, electrons can hop easily out of the sites with low free energy barriers in the direction of the electric field and tend to accumulate at sites of high free energy barriers. This can lead to a net polarization of the dielectric medium and consequently, to higher dielectric values [19]. However, at high frequency the charge carriers will no longer be able to relax as rapidly as the time variation of the field, so the charge oscillation will begin to lag behind this field, resulting in a decrease of dielectric constant [20].

The loss tangent, tan δ (which is a measure of the dissipated energy in the sample), was measured for the synthesized sample over the same range of frequency and temperature used for dielectric constant. The imaginary part of the dielectric function was estimated according to the relation:

$$\varepsilon'' = \varepsilon' \tan \delta$$

Figure 7b displays the variation of the dielectric loss, ε'', of the sol-gel synthesized sample on the applied frequency at different temperatures. It is evident that there is a strong frequency dependence of ε''. From the calculated dielectric loss, ε'' decreases with the increase in frequency at all studied temperatures. The calculated dielectric loss, ε'' decreases with frequency increase at all temperatures, with no relaxation peaks which may be due to the small grain size of $SrTiO_3$ which facilitates the polarization of the molecule.

The values of dielectric constant of $SrTiO_3$ prepared by the sol-gel technique are higher than those of the samples prepared by the solid state method, Fig. 8a. Additionally, the dielectric constant of $SrTiO_3$ prepared by solid state is independent on temperature.

Additionally, the dielectric loss of SrTiO3 prepared by solid state is independent of temperature, Fig. 8b.

4 Conclusions

The synthesis of strontium titanate $SrTiO_3$ nanopowders by two different methods namely, sol-gel and solid state methods, is shown. The powder obtained by the solid state method was mainly $SrTiO_3$ whereas $SrTiO_3$ with anatase TiO_2 was obtained by the sol-gel method. The solid state synthesis of $SrTiO_3$ leads to the formation of heterogeneous microcrystalline particles, while the employed sol-gel approach leads to the formation of homogenous nanoparticles with sizes in the nanometer regime. The magnetization and the dielectric characteristics of the synthesized $SrTiO_3$ were investigated. The sol-gel synthesized sample shows a higher magnetization compared with the solid state synthesized one. The samples obtained by the sol-gel method exhibit higher dielectric values than those of the samples prepared by the solid state method.

Acknowledgements This work was supported by the National Research Centre through the grant number 11090313.

References

1. Cardona M (1965) Phys Rev 140:651
2. Luo J, Maggard P (2006) Adv Mater 18:514
3. Liu J, Chena G, Lia Z, Zhang Z (2006) J Solid State Chem 179:3704
4. Jia L, Urban K, Hoffmann S, Waser RJ (1998) Mater Res 13:2206
5. Kolodiazhnyi A, Petric A (2005) J Electroceramics 15:5
6. Abe K, Komatsu S (1995) J Appl Phys 77:6461
7. Shibuya M, Nishitsuji M, Kitagawa M, Kamada T, Hayashi S, Tamura A, Hirao T (1993) Jpn J Appl Phys 32:L1830
8. Selvaraj U, Prasadarao AV, Komarneni S, Roy R (1995) Mat Lett 23:123
9. Tagawa H, Igarashi K (1986) J Am Ceram Soc 69:310
10. Trepakov VA, Savinov ME, Okhay I, Tkach A, Vilarinho PM, Kholkin AL, Gregora I, Jastrabik L (2007) J Eur Ceram Soc 27:3705
11. Fukushima K, Shibagaki S (1998) Thin Solid films 315:238
12. Yu T, Chen YF, Liu ZG, Ming NB, Wu XS (1999) Appl Surf Sci 138/139:605
13. Pang Q, Shi JX, Gong ML (2007) J Am Ceram Soc 90:3943
14. Dutta PK, Gregg JR (1992) Chem Mater 4:843
15. Um M-H, Kumazawa H (2000) J Mater Sci 35:1295
16. Klaytae T, Panthong P, Thountom S (2013) Ceram Int 39:S405
17. Zhi Y, Chen A, Vilarinho PM, Mantas PQ, Baptista JL (1998) J Appl Phys 83:4874
18. Kumar MP, Saukarappa T, Kumar S (2008) J Alloys Compd 464:393
19. Kumar RS, Haran K (1999) Mat Chem Phys 60:11
20. Bergo P, Pontuschka WM, Prison JM, Motta CC, Martinelli JR (2004) J Non-Cryst Solids 348:84